AIAA 80-0208R

Turbulence-Generated Pressure Fluctuations in a Rocket-Like Cavity

Warren C. Strahle* and Douglas H. Neale†
Georgia Institute of Technology, Atlanta, Ga.

Theoretical acoustics applied to the pipe flow turbulence problem in a configuration that was experimentally investigated yields an analytical formula for random pressure fluctuations generated by the turbulence. In order to calculate the pressure fluctuations, it is found that certain spatial correlations of the fluctuation in the square of the axial velocity are needed. These are measured by hot-film anemometry, as are the pressure fluctuations, in a fully developed pipe flow and the theory is shown to be semiquantitative; a lower bound to the pressure fluctuation emerges. Application to the problem of pressure fluctuations in rocket motors and attendant vibration are indicated.

Nomenclature

A = pipe cross-sectional area
A_{cor} = correlation area of turbulence
a = pipe radius
c = speed of sound
f = quantity defined by Eq. (6)
g_ω = Green's function for plane wave acoustics problem
g = Green's function for H
H = Bernoulli enthalpy
J_m = Bessel function of order m
ℓ = duct length
ℓ_{cor} = axial correlation length scale of turbulence
n = outward unit normal vector
p = pressure
S_{ij} = cross-spectral density between signal i and signal j
S_{II} = cross spectrum of pressure due to local turbulence
S_{IIII} = cross spectrum of pressure due to propagational sound
s_{mn} = eigenvalue in the problem for H
s = entropy
t = time
t_0 = sample time in Fourier transform
u = vortical velocity vector
V = volume
v = velocity vector
w = potential velocity vector
x_i = Cartesian coordinate in ith direction
x = distance along duct
x_0 = distance along duct
V_{cor} = correlation volume for turbulence
β = quantity defined by Eq. (8)
δ = Dirac delta function
ρ = density or probe separation distance
ω = radian frequency
φ = velocity potential

Subscripts

t = transverse part
oo = plane approximation
cor = correlation scale
∞ = value at infinity in the potential field
ω = Fourier transform
1 = x direction

Superscripts

$(\ )'$ = fluctuation
$(\bar{\ })$ = mean or ensemble average

Presented as Paper 80-0208 at the AIAA 18th Aerospace Sciences Meeting, Pasadena, Calif., Jan. 14-16, 1980; revision received Sept. 2, 1980.

*Regents' Professor, School of Aerospace Engineering. Associate Fellow AIAA.
†Senior Research Engineer, School of Aerospace Engineering.

Introduction

PRESSURE fluctuations inside of a rocket motor cavity are one source of motor vibrations. Typically, the broadband random pressure fluctuations which are normally considered reasonable to tolerate are of the order of 1% rms magnitude when compared with the mean chamber pressure. Depending upon the frequency content of this background noise in the pressure, however, this 1% level can cause vibration troubles. Especially if the excitation frequencies overlap a longitudinal mode frequency of the chamber cavity, strong longitudinal resonances may occur with attendant thrust fluctuations. Such fluctuations in thrust can be more than the 1% level of the pressure fluctuations because the pressure field is spatially variant and differentially acts on the head and aft ends of the cavity. This kind of problem is currently believed to exist in one large system.[1]

There are several potential sources for the background pressure fluctuations, and many of these have been considered in Ref. 2. However, the results of Ref. 2 contain an ambiguity in interpretation due to the simplified theory employed, and it is desirable to use a more accurate theory to treat the problem. The approach here is to look at the problem of turbulence induced pressure fluctuations, both theoretically and experimentally, with a view towards prediction of the pressure fluctuation level in rocket motors, due to the turbulence field. There will necessarily be left out, at this point, other potential sources of vibration such as combustion noise.[2]

The approach here is to first look at a relatively well-characterized turbulence field, that of pipe flow, encountering a rocket-like flow termination, that of a choked deLaval nozzle. The purpose is to see the accuracy with which the pressure fluctuation levels may be predicted by theory, given appropriate measurements of the turbulence field. If satisfactory answers may be obtained, the theory may be applied to rocket motors as further information becomes available on the rocket motor turbulence field, as given, for example, by the computations of Ref. 3. For the moment, however, this may be regarded as a fundamental investigation of turbulence generated pressure fluctuations in a given type of interior flow problem.

Analysis

Consider the configuration of Fig. 1, where a pipe flow is terminated by a choked nozzle and is also the configuration in the experimental results to follow. Except very near the walls the inlet flow is nearly potential; there follows a transition to

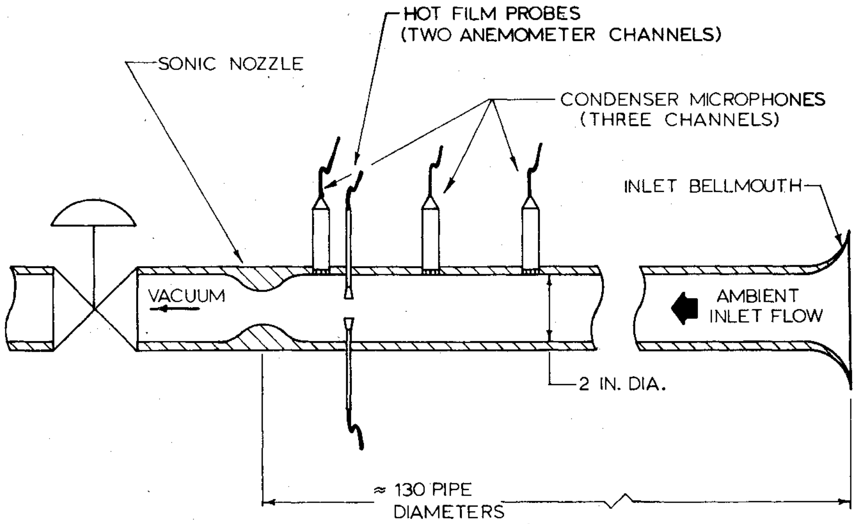

Fig. 1 Schematic drawing of the experimental configuration.

turbulent flow and finally a fully-developed purely vortical turbulent pipe flow. In the fully-developed turbulent region it is the mean flow that is purely vortical, but superimposed is a turbulent fluctuation that has pressure fluctuations associated with it. The calculation of the pressure field is the issue here.

Consider the formulation of the conservation equations as given by Yates and Sandri.[4]

$$\frac{D}{Dt}\left(\frac{\partial \varphi}{\partial t}+\frac{|\nabla\varphi|^2}{2}\right)-c^2\nabla^2\varphi=\frac{DH}{Dt} \tag{1}$$

$$\nabla^2 H=-\frac{\partial^2 u_i u_j}{\partial x_i \partial x_j}-\frac{\partial^2}{\partial x_i \partial x_j}\left(u_j\frac{\partial \varphi}{\partial x_i}\right)-\frac{\partial}{\partial x_j}\left(\frac{\partial u_j}{\partial x_i}\frac{\partial \varphi}{\partial x_i}\right) \tag{2}$$

$$v=w+u \qquad w=\nabla\varphi \qquad \nabla\cdot u=0 \tag{3}$$

$$s=s(p,h)=s_0=0=\ln\frac{h}{h_0}-\frac{\gamma-1}{\gamma}\ln\frac{p}{p_0} \tag{4}$$

In the preceding, all effects of viscosity and heat conduction are neglected so that when considering fluctuations it is understood that the frequency domain under consideration is that of the energy containing eddies of the turbulent flow. The isentropic specialization has also been made in the more general formulation of Ref. 4, consistent with the neglect of transport phenomena and the further assumption of no chemical reactions. A companion equation to Eq. (2) has been omitted; it is the vorticity conservation equation. H is the Bernoulli enthalpy given by

$$H=h+\frac{\partial\varphi}{\partial t}+\frac{|\nabla\varphi|^2}{2} \tag{5}$$

and plays a fundamental role in the generation of noise in Eq. (1). In the potential flow region of the pipe flow $\nabla^2 H=0$ and $H=H_\infty$, a constant. In the fully-developed pipe flow region such a relation does not hold, but Eq. (2) must be solved. It will be assumed, and has been experimentally checked, that the majority of the experimental configuration is filled with the fully-developed pipe flow so that Eq. (2) is to be solved.

The preceding formulation is currently preferred by the authors, as opposed to several other possible aeroacoustics formalisms that are possible in order to treat the problem. It will be found that the potential field of Eq. (1) is driven by the creation of Bernoulli enthalpy by the first term on the right-hand side of Eq. (2). This will clearly establish the vortical part of the velocity field as the culprit in noise generation. This will remove the ambiguity in Ref. 2, which used a Lighthill approach. The final results will turn out to be equivalent to a Ribner[5] formalism, but, again, an ambiguity is removed in that the vortical field is clearly identified as the noise source. This point is clearly covered in Ref. 4. Moreover, there are advantages to this formalism when chemical reaction is considered, which is a desired future extension of this work.

It is assumed that the potential velocities are much less than the vortical velocities, which has been verified after the fact, so that Eq. (2) becomes

$$\nabla^2 H=-\frac{\partial^2}{\partial x_i \partial x_j}(u_i u_j)\equiv -f(x_i,t) \tag{6}$$

The genesis of Eq. (2) is the momentum equation

$$\nabla H=\nabla\left(\frac{|\nabla\varphi|^2}{2}\right)-\frac{\partial u}{\partial t}-v\cdot\nabla v \tag{7}$$

which is zero on the walls of the tube because all velocities must vanish. At the head end of the tube $\nabla H=0$ since the flow is a potential flow. At the nozzle end, however, more care is required. What is needed to solve Eq. (6) is the boundary condition $\nabla H\cdot n$ on all boundaries of the flow region.

Splitting the velocity into its mean plus fluctuating components and noting that at the nozzle end $\nabla\bar{\varphi}=0$ and $\bar{v}=u_1(r)$, the $x_1=x$ component of Eq. (7) becomes

$$\nabla H\cdot i=-\frac{\partial u_1}{\partial t}-u\cdot\nabla u_1\equiv\beta \tag{8}$$

In Eq. (8) the fluctuations in the potential field have been neglected as compared with those in the vortical (turbulence) field.

Now it is presumed that the vortical field is known or can be measured so that the right-hand sides of Eqs. (6) and (8) are known. The solution may be written in terms of the Green's function for the Poisson equation

$$\nabla^2 g(x_i,x_{0_i})=-\delta(x_i-x_{0_i})$$

$$\nabla g\cdot n=0 \text{ on the side wall and exit plane}$$

$$g=0 \text{ at the entrance plane} \tag{9}$$

whereby

$$H-H_\infty=\int_V g(x_i,x_{0_i})f(x_{0_i})\mathrm{d}V_0+\int_{A_e} g\beta \mathrm{d}A_0 \qquad (10)$$

The Green's function may be constructed by standard methods and is given by

$$g=\sum_{m,n=0}^{\infty} F_{mn}(x,x_{0_i})J_m(s_{mn}r)^{\cos m\Theta}_{\sin m\Theta} \qquad (11)$$

where F_{mn} satisfies

$$\frac{\mathrm{d}^2}{\mathrm{d}x^2}F_{mn}-s_{mn}^2F=-\frac{\Theta(\Theta_0)J_m(s_{mn}r_0)\delta(x-x_0)}{\pi a^2\Lambda_{mn}}$$

$$\Lambda_{mn}=\frac{1}{\mathcal{E}_m}\left[1-\frac{m^2}{(s_{mn}a)^2}\right]J_m^2(s_{mn}a)$$

$$\mathcal{E}=1 \text{ if } m=0$$
$$=2 \text{ if } m\geq 1$$

and s_{mn} is determined by

$$s_{mn}J'_m(s_{mn}a)=0$$

The term in the solution with $m=n=0$ has only an axial dependence and corresponds to cross-sectional averages of quantities. Emphasizing this,

$$g=g_{oo}+g_t \qquad H-H_\infty=H_{oo}+H_t-H_\infty$$

where the t subscript denotes the part which is due to transverse dimensions of the duct.

The crucial step is now taken to ignore the higher terms in g other than g_{oo}. It will be argued later that this will yield a lower bound on the pressure generated by the turbulence. Constructing g_{oo}, from Eqs. (9), it is found,

$$g(x,x_0)=g_{oo}=-\frac{x}{\pi a^2} \qquad x_0\geq x$$

$$g(x,x_0)=g_{oo}=-\frac{x_0}{\pi a^2} \qquad x_0\leq x \qquad (12)$$

The fluctuation in H, $H'=H_{oo}-H_\infty$, is then constructed from Eq. (10) after considerable manipulation and noting that $\nabla\cdot u=0$. The result is

$$H'=\frac{1}{A}\int \mathrm{d}A(u_1u_1)' \qquad (13)$$

This result, remarkable in its simplicity, says that Bernoulli enthalpy fluctuations merely are created by the fluctuations in the square of the vortical part of the axial velocity components.

Now moving to construction of the unsteady potential field, it is readily shown that for low Mach number, which is assumed and corresponds to the experimental situation, and sufficiently small fluctuations in the potential field, which has already been assumed, Eq. (1) reduces to

$$\frac{\partial^2\varphi'}{\partial t^2}-\bar{c}^2\nabla^2\varphi'=\frac{\partial H'}{\partial t} \qquad (14)$$

Since H' is purely planar by the preceding developments, a plane wave solution to Eq. (14) is adequate. After taking the Fourier transform of Eq. (16), the solution is

$$\varphi_\omega=\frac{i\omega}{A\bar{c}^2}\int \mathrm{d}V(x_0)g_\omega(x,x_0)\int \mathrm{d}A(u_1u_1)'_\omega \qquad (15)$$

where g_ω is the plane wave Green's function for the duct. It, again, may be constructed by standard means and depends upon the impedance of the duct walls and end planes. If, as in the experiment, it may be assumed that the walls are hard, the open end is like an open ended organ pipe and the nozzle end behaves like a hard wall,[6] an especially simple form for g_ω emerges. It is

$$g_\omega=\frac{\sin k(\ell-x_0-x)+\sin k(\ell-x_0+x)}{2k\cos k\ell} \qquad x<x_0$$

$$g_\omega=\frac{\sin k(\ell+x_0-x)-\sin k(x_0-\ell+x)}{2k\cos k\ell} \qquad x\geq x_0 \qquad (16)$$

Since all terminations and walls were assumed perfectly reflecting, Eq. (16) contains resonances of infinite magnitude. It is not hard to show, however, that Eq. (16) is valid around the troughs even when the walls are nearly perfectly reflecting. Equation (16) will be used, therefore, away from the resonance frequencies.

Finally, the linearized, low Mach number form of the equation of state, Eq. (4), using Eq. (5) becomes

$$p'=\rho_0\left(H'-\frac{\partial\varphi'}{\partial t}\right), \qquad p_\omega=\rho_0(H_\omega+i\omega\varphi_\omega)$$

Using this with Eqs. (13) and (15), the final relation for the pressure transform becomes

$$p_\omega(x)=\rho_0\frac{1}{A}\int \mathrm{d}A(u_1u_1)'_\omega+\rho_0\frac{k^2}{A}\int \mathrm{d}x_0g_\omega(x,x_0)$$
$$\times\int \mathrm{d}A_0(u_1u_1)'_\omega$$
$$\equiv I+II \qquad (17)$$

The pressure fluctuation therefore consists of two superimposed parts. I is a local noise due to the local turbulence field. II is a propagational sound, because of the appearance of g_ω, and is the sound pumped up by the entire volume of turbulence. The frequency content of I is the frequency of the square of the axial velocity fluctuation, and that of II is modified by g_ω.

Now consider the construction of the cross spectral density of a pressure at two different points, x_1 and x_2. Using Eq. (17),

$$S_{12}=S_{I(x_1)I(x_2)}+S_{I(x_1)II(x_2)}+S_{II(x_1)I(x_2)}+S_{II(s_1)II(x_2)}$$

Using the notation $T_\omega(x)=(u_1u_1)'_\omega$, it is seen

$$S_{I(x_1)I(x_2)}=\frac{\rho_0^2}{A^2}\frac{\overline{(\int \mathrm{d}AT^*_\omega(x_1))(\int \mathrm{d}AT_\omega(x_2))}}{t_0}$$

But if x_1 and x_2 are separated sufficiently there is expected no correlation between $T_\omega(x_1)$ and $T_\omega(x_2)$ so $S_{I(x_1)I(x_2)}\approx 0$. On the other hand, if $x_1=x_2$, so that an autospectrum of the pressure is considered, S_{II} is nonzero and is given by

$$S_{II}=\left(\frac{\rho_0}{A}\right)^2\int \mathrm{d}A(r,\Theta)\int \mathrm{d}A(\tilde{r},\tilde{\Theta})\frac{\overline{T^*_\omega(x,r,\Theta)T_\omega(x,\tilde{r},\tilde{\Theta})}}{t_0} \qquad (18)$$

Investigation of the magnitude of Eq. (18) reveals that it is expected to be of order

$$S_{II} \text{ is } \mathcal{O}[S_{TT}\rho_0^2 A_{\text{cor}}/A]$$

Similar manipulations on $S_{II(x_I)II(x_2)}$ yield that even when x_I and x_2 are separated there is correlation between the signals due to the fact that II corresponds to propagational sound. In fact,

$$S_{II(x_I)II(x_2)} = \frac{\rho_0^2 k^4}{A^2}\int_0^\ell \mathrm{d}x_0 \int_0^\ell \mathrm{d}\tilde{x}_0 g_\omega^*(x_I,x_0) g_\omega(x_2,\tilde{x}_0)$$

$$\times \int_A \mathrm{d}A(r,\Theta) T_\omega^*(x_0,r,\Theta) \int_A \mathrm{d}A(\tilde{r},\tilde{\Theta}) T_\omega(\tilde{x}_0,\tilde{r},\tilde{\Theta}) \quad (19)$$

The point is that both x_0 and $\tilde{x}_0$ run from 0 to ℓ to where $x_0 \approx \tilde{x}_0$ the T values are correlated. Careful examination yields the order of magnitude result

$$S_{II(x_I)II(x_2)} \text{ is } \mathcal{O}[\rho_0^2 k^4 S_{TT} V_{\text{cor}} \ell |g_\omega|^2]$$

Consider $x_I = x_2$, so an autospectrum is being considered, and the ratio of S_{II} to $S_{II\,II}$ is

$$\frac{S_{II}}{S_{II\,II}} \text{ is } \mathcal{O}\left[\frac{\cos k\ell A_{\text{cor}}}{k^2 V_{\text{cor}} \ell}\right]$$

The exact nature of this ratio depends upon the behavior of the correlation area and volume with frequency, but generally it is expected that 1) the propagational sound may dominate near resonance peaks ($\cos k\ell \approx 0$) and 2) away from resonance S_{II} will dominate since $k\ell$ is of order unity or larger but $kV_{\text{cor}}/A_{\text{cor}}$ is roughly like

$$k\ell_{\text{cor}} \approx \omega a/c \approx (\omega a/\bar{u})(\bar{u}/c) \ll 1$$

for low Mach number flows with turbulence centered about frequencies $\omega a/\bar{u} \approx 1$. It may further be shown that the cross terms $S_{I\,II}$ and $S_{II\,I}$ are small compared with either S_{II} or $S_{II\,II}$. Consequently, the situation is as follows: 1) If x_I and x_2 are widely separated only $S_{II\,II}$ should be sensed by a cross spectrum of two pressure transducers. 2) If $x_I = x_2$ the autospectrum of the pressure will contain mainly $S_{I\,I}$ with contamination by $S_{II\,II}$ at resonant frequencies. 3) If enough information is available on the spatial correlation of T_ω the pressure should be calculable.

It is argued that the pressure computed from Eq. (17) is a lower bound to the actual pressure. This conjecture is due to the retention of only one term, the plane approximation, in H'. Actually, the Green's function of Eq. (11) contains an infinite number of terms. However, each term is somewhat uncorrelated with every other term because of different transverse function weighting in the integration operation of Eq. (10). Consequently, the mean square pressure should consist mainly of a sum of squared terms, the first of which is given by the solution as given here. Further work in completion of such a solution to include transverse dependence of g should be carried out.

Experimental

The tube of Fig. 1 is 6.1 m long, 5.08 cm in diameter, and instrumented with flush mounted microphones and hot-film anemometers. Because $(u_I u_I)'$ is desired from the hot films, the individual signals are first passed through a linearizer, then squared, and then filtered to remove the dc part. All signals are recorded on magnetic tape for later Fourier analysis.

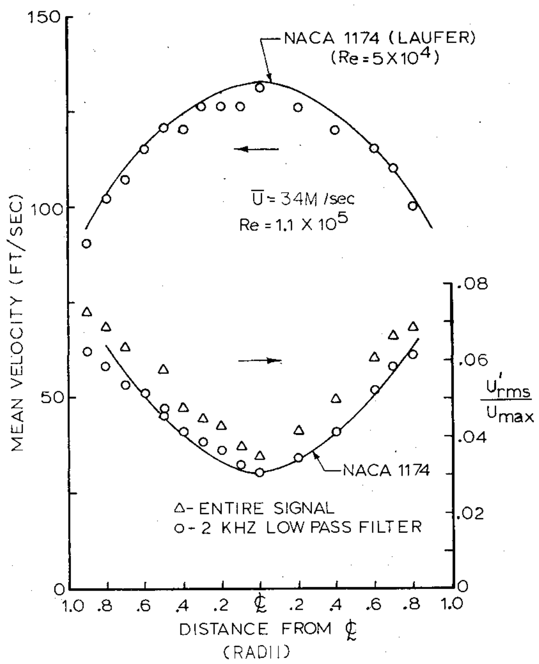

Fig. 2 Comparison of Laufer's pipe flow data with that obtained in the current experimental configuration.

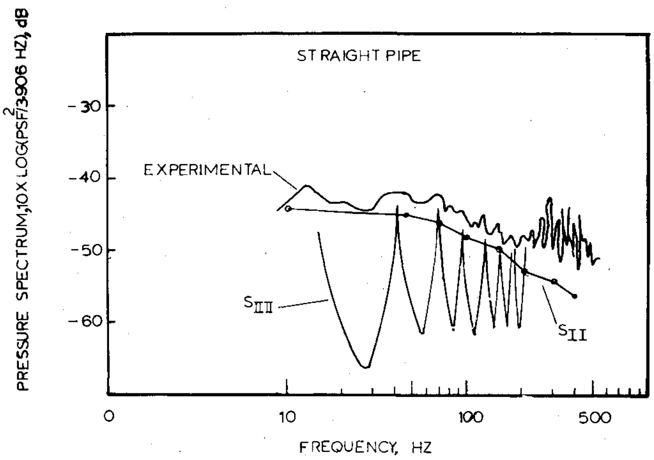

Fig. 3 Measured pressure spectrum at the wall and at the nozzle entrance plane. Calculated contributions to the pressure from the velocity fluctuation data.

The nozzle for most runs has a contraction ratio to give an average Mach number of 0.1 at the entrance plane. To insure fully-developed pipe flow by this station measurements were made of the mean velocity and axial turbulence intensity. These measurements are shown in Fig. 2 and are compared with Laufer's[7] pipe flow data. The axial extent of the fully developed flow was determined to be essentially the last three quarters of the tube length.

First consider the pressure autospectrum shown in Fig. 3. The pressure is here being measured 5.1 cm upstream of the nozzle. The spectrum consists of a broadband noise on which there are superimposed weak resonance peaks at the ¼ wave resonance points. This is the situation expected from the preceding theory. Figure 4 displays the cross-spectral density magnitude between two microphones placed 20.3 cm apart. Clearly what has been done is to suppress $S_{I(x_I)\,I(x_2)}$, as expected, and to reveal only the propagational sound. These observations are in accord with the qualitative expectations from theory; the question now is the quantitative agreement.

To see if the pressure is calculable, what is needed for S_{II} is given in Eq. (18). Using the cylindrical coordinate system of

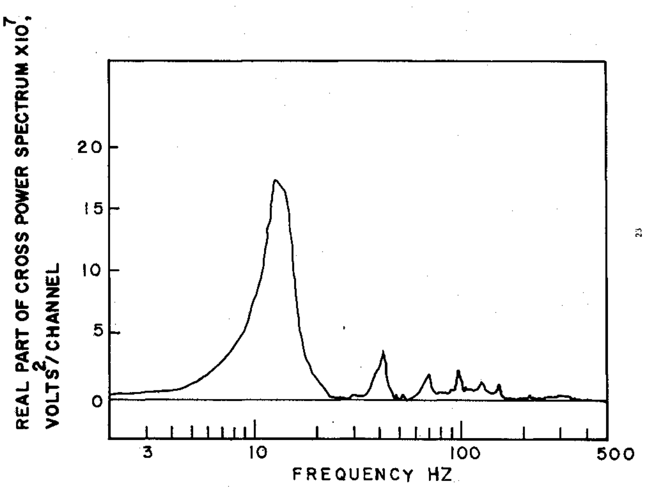

Fig. 4 Cross-spectral density between two microphones separated by 20.8 cm.

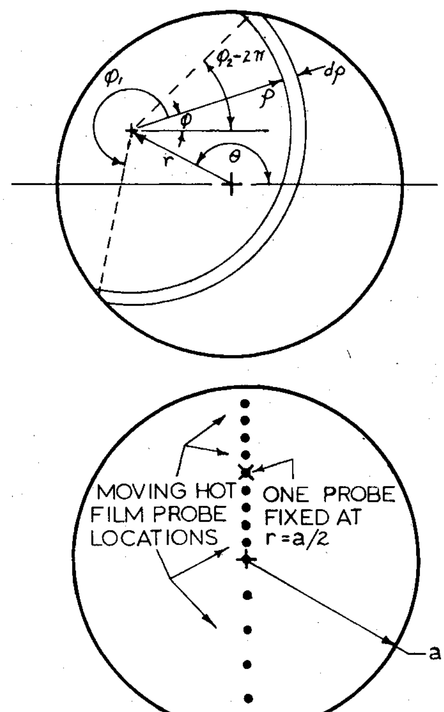

Fig. 5 Coordinate system for spacewise cross correlations of velocity fluctuations and actual experimental points.

Fig. 5, this becomes

$$S_{II}=\frac{\rho_0^2}{A^2}\int \mathrm{d}A(r,\Theta)\int_0^{2a}\mathrm{d}\rho\int_{\varphi_1(\rho,r,\Theta)}^{\varphi_2(\rho,r,\Theta)}\mathrm{d}\varphi\rho S_{T(r,\Theta)T(r,\Theta,\rho,\varphi)}$$

While axial symmetry helps somewhat, this still requires an enormous number of cross-spectral densities of space separated hot films to obtain accurate numbers. Accordingly, an approximate procedure is used. A representative r, Θ point is taken as $r=a/2$, $\Theta=\pi/2$ and a fixed anemometer is placed at this point. A traverse of separation distance $\rho=0$ to $a/2$ is taken with $\varphi=\pi/2$ and then a traverse $\rho=0$ to $3a/2$ is made with $\varphi=3\pi/2$. $S_{I\,I}$ is then approximated by numerical integration of the results.

$$S_{II}\approx\frac{\rho_0^2}{A}2\pi\left[\left(\int_0^{a/2}S_{TT}\right)_{\varphi=\pi/2}\rho\mathrm{d}\rho+\left(\int_0^{3a/2}S_{TT}\right)_{\varphi=3\pi/2}\rho\mathrm{d}\rho\right]$$

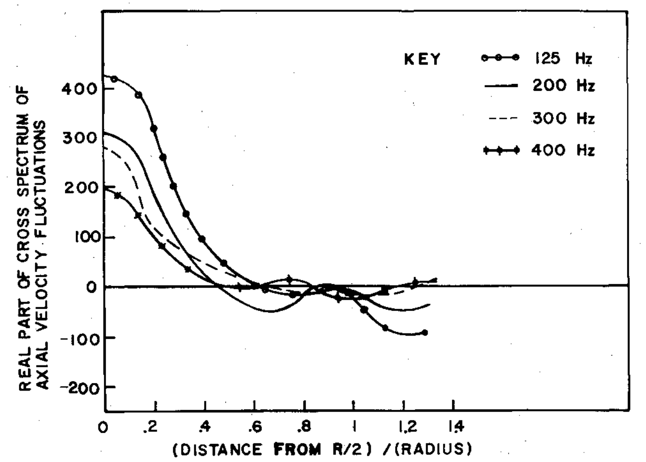

Fig. 6 Cross-spectral density of transversely separated hot-film anemometers for various frequencies.

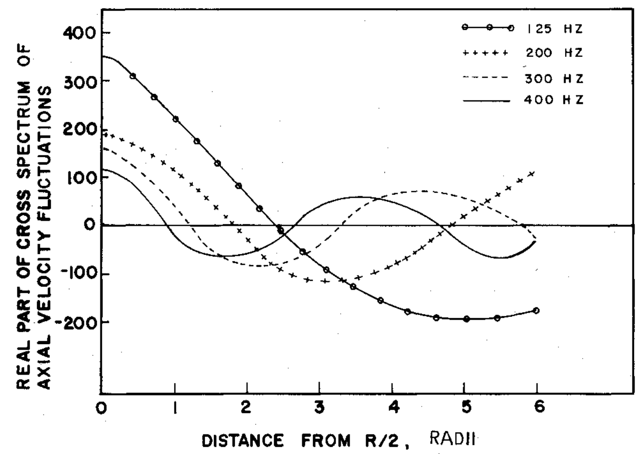

Fig. 7 Real part of cross-spectral densities of axially separated hot-film anemometers for various frequencies.

Shown in Fig. 6 is the behavior of S_{TT} as a function of separation distance ρ for various frequencies. As expected, the size scale over which neighboring anemometers are correlated decreases with an increase in frequency. S_{II} is then calculated by integration and the result is shown on Fig. 3. It is seen that 1) indeed a lower bound is produced for the broadband noise, 2) the frequency content is roughly correct, and 3) this lower bound is only about 2 dB lower than the experimental curve (that is, the theory underestimates the actual linear rms pressure by about a factor of 1.6).

$S_{II\,II}$ is more difficult to come by because there is an axial integration also involved in Eq. (19). Looking at the autospectrum, letting $x_0=x_0+\zeta$, and assuming the Green's function varies slowly over the distance scale where the axial correlation of T drops to zero, there results the approximation

$$S_{II\,II}=\frac{\rho_0^2}{A^2}k^4\int \mathrm{d}x_0 g_\omega^*(x,x_0)g_\omega(x,x_0)\int_{-\infty}^{\infty}\mathrm{d}\zeta\int \mathrm{d}A(r,\Theta)$$

$$\times\int \mathrm{d}A(\rho,\varphi)S_{T(x_0,r,\Theta(T(x_0+\zeta,\delta,\Theta,\rho,\varphi)}$$

The difficulty here is that now S_{TT} has a phase, dependent on ζ, because of convection of disturbances. However, $S_{II\,II}$ is real so that the integration must cancel out all phase. Consequently, only the real part of S_{TT} is used in the preceding. A typical example of $S_{T(x_0,r,\Theta)T(x_0+\zeta,r,\Theta)}$ is shown in Fig. 7. The

Table 1 Scaling of pressure level with flow velocity

Mass weighted flow velocity, m/s	Sound pressure level dB re 2×10^{-5} n/m^2)
34.1	108.5
49.4	111.8
65.2	115.8

prior formula is estimated by

$$S_{II\,II} = S_{II} k^4 \ell_{cor} \int_0^{\ell} |g_\omega|^2 dx_0$$

where

$$\ell_{cor} = \frac{1}{S_{TT}} \int_{-\infty}^{\infty} S_{T(x_0,r,\Theta)T(x_0+\zeta,r,\Theta)} d\zeta \qquad (20)$$

and the integral is numerically computed from the data. This is clearly a rather coarse estimate, and, recall, the Green's function is not accurate near the resonance peaks. The calculation of Eq. (20) is shown near the troughs in g_ω on Fig. 3. Again, a lower bound is evident and the troughs, as expected, are significantly down from the lower bound estimate of S_{II}.

In the experimental configuration, the S_{II} term is dominating the pressure fluctuation. Integration of the spectrum to yield the mean square pressure is made difficult because of the A_{cor} term in the order of magnitude estimate below Eq. (19). If A_{cor} were independent of frequency

$$\langle p'^2 \rangle \propto \bar{U}^4$$

would result. However, since A_{cor} may be expected to fall with frequency, a dependence on $\bar{U}$ to somewhat less than the fourth power would be expected. Checking this with nozzles of differing contraction ratio, the results is shown in Table 1. The result is that $\langle p'^2 \rangle \propto \bar{U}^3$.

Concluding Remarks

What has now been gained is an understanding of the pressure fluctuation generation by turbulence in an interior flow. This understanding is semiquantitative in the sense that a lower bound to the pressure field may be calculated from knowledge of spatial correlations of the turbulence velocities. The next step would be to use information on rocket motor turbulence, if available, together with an accurate calculation of g as, for example, in Ref. 2, and to use these pieces of information to calculate pressure fluctuations in a rocket motor cavity. The problem is that the necessary correlations are not available. While progress is being made in calculation of the kinetic energy of turbulence[3] the spatial correlations necessary here do not appear to be forthcoming. Consequently, current work is centering on measurement of the necessary turbulence quantities in a tube as in Fig. 1 but with blowing from the side walls, to simulate a solid rocket cavity.

Acknowledgments

This work was supported by the Air Force Office of Scientific Research under Contract FA9620-78-C-0003. Mr. R. Christiansen gave invaluable help during the data reduction portion of the program.

References

[1] Mathes, H. B., "Assessment of Chamber Pressure Oscillations in the Shuttle SRB," 16th JANNAF Combustion Meeting, Monterey, Calif., Sept. 1979.

[2] Strahle, W. C. and Handley, J. C., "Prediction of Combustion Induced Vibration in Rocket Motors," Final Rept. U. S. Army Contract DASG60-77-C-0054, April 1978.

[3] Beddini, R. A. and Varma, A. K., "The Erosive Burning of Ammonium Perchlorate," 16th JANNAF Combustion Meeting, Monterey, Calif., Sept. 1979.

[4] Yates, J. E. and Sandri, G., "Bernouli Enthalpy: A Fundamental Concept in the Theory of Sound," *Aeroacoustics: Jet Noise, Combustion and Core Engine Noise,* edited by I. R. Schwarz, MIT Press, 1976, p. 65.

[5] Ribner, A. S., "The Generation of Sound by Turbulent Jets," *Advances in Applied Mechanics,* edited by Dryden and von Karman, Academic Press, New York, 1964, pp. 103-182.

[6] Crocco, L. and Sirignano, W. A., "Behavior of Supercritical Nozzles under Three Dimensional Oscillatory Conditions," AGARDograph 117, 1967.

[7] Laufer, J., "The Structure of Turbulence in Fully Developed Pipe Flow," NACA TR1174, 1957.